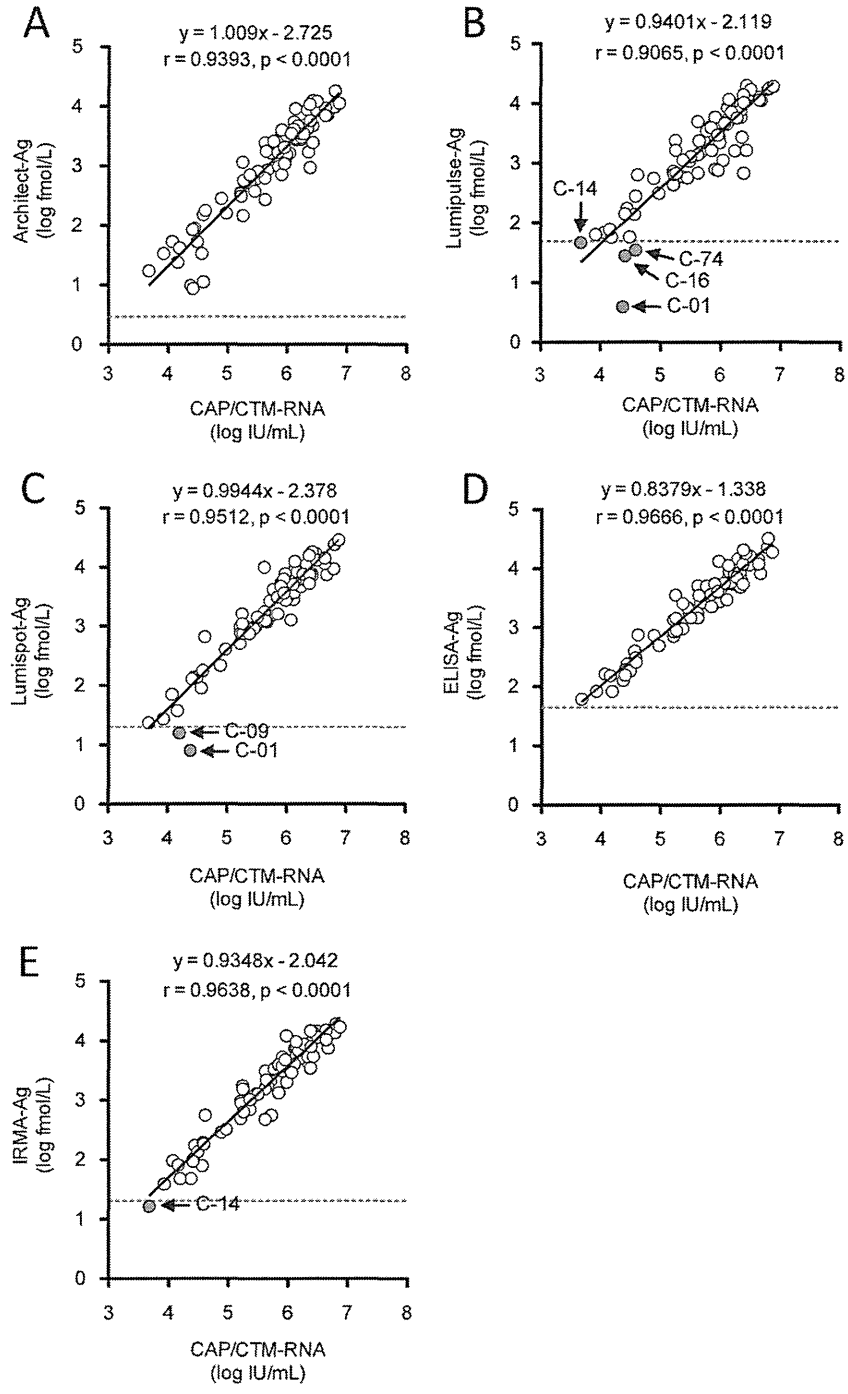

FIG 2 Correlation between CAP/CTM-RNA and core Ag levels as quantified by five commercial kits. Data for core Ag levels were converted to log fmol/liter prior to analysis. In each plot, the lower limit of detection of the respective core Ag assay is indicated by a dotted line. Data for samples below the lower detection limit of each assay are indicated by shaded circles labeled with the respective sample designations.

specifically an Arg-to-Gly substitution at aa 47. We suspected that these polymorphisms altered the antigenicity of the core protein, thereby reducing detected core Ag levels and leading to underestimation of values by the core Ag quantification kits. To assess the correlation of these polymorphisms with the underestimation of core Ag values, strains containing polymorphisms in this region (at aa 47 to 49 [Fig. 4]) were identified in Bland-Altman plots of HCV RNA and core Ag (Fig. 3; also, see Fig. S2 in the supplemental material). A total of 12 strains exhibited polymorphisms at these positions, including 2 strains of genotype 1b, 8 of genotype 2a, and 2 of genotype 2b (Table 1). In the Bland-Altman plot of CAP/CTM-RNA and Architect-Ag, 4 of 12 values (for samples C-01, C-16, C-73, and C-74) were located under the line of the lower 95% limit of agreement (Fig. 3A). Likewise, in the plot of CAP/CTM-RNA and Lumipulse-Ag, 3 of 12 values (those for samples C-01, C-67, and C-73) were located under the line of the lower

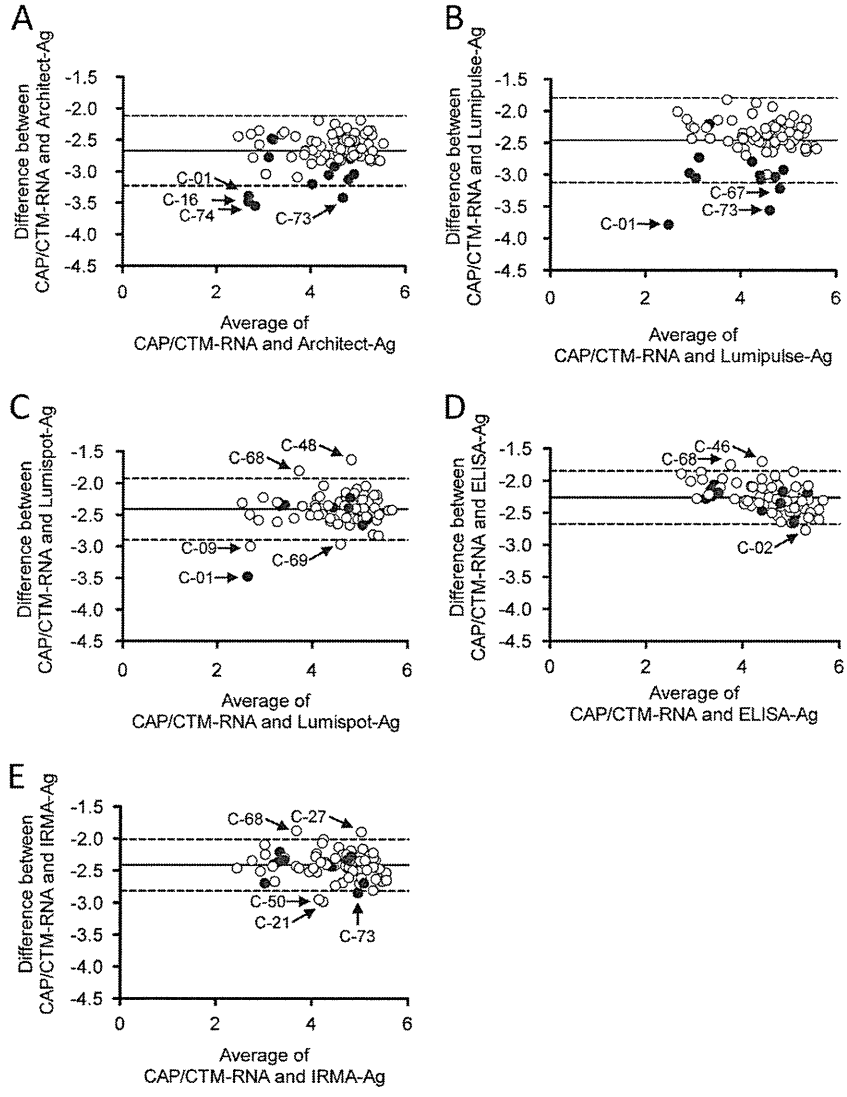

FIG 3 Bland-Altman plot analysis of CAP/CTM-RNA and core Ag levels as quantified by five commercial kits. These plots show the difference between the values of HCV RNA and core Ag as a function of the average of these two values. Data for core Ag levels were converted to log fmol/liter prior to analysis. The bias and 95% limits of agreements are indicated by solid and dashed lines, respectively. Data for samples with polymorphisms at amino acid residues 47 to 49 are indicated by solid circles. Data points outside the 95% limits are indicated by arrows labeled with the sample designations.

95% limit of agreement (Fig. 3B). In these plots, underestimation for samples that lacked these polymorphisms (at aa 47 to 49) was not detected. In the plot of CAP/CTM-RNA and Lumispot-Ag, only 1 sample (C-01) was located under the line of the lower 95% limit of agreement, but this sample exhibited the most discordant value (Fig. 3C). In the plot of CAP/CTM-RNA and ELISA-Ag, no correlation between polymorphisms at these positions and underestimation was observed (Fig. 3D). In the plot of CAP/CTM-RNA and IRMA-Ag, sample C-73 was located under the line of the lower 95% limit of agreement, as were other samples that lacked polymorphisms at aa 47 to 49 (Fig. 3E). Similar trends were observed in comparison with ART-RNA levels (see Fig. S2 in the supplemental material). Based on these results, the levels of HCV core Ag measured with Architect-Ag and Lumipulse-Ag seem to be more strongly affected by single polymorphisms at these positions. In the case of Lumispot-Ag, underestimation may be limited to specimens with multiple polymorphisms at these positions.

TABLE 1 Number of reference panel strains with polymorphisms at amino acid residues 47 to 49 of the HCV core region

Genotype	No. (%) of strains	
	Total	With polymorphisms
1a	1	0
1b	35	2 (5.7)
2a	26	8 (30.8)
2b	18	2 (11.8)
Total	80	12 (15.0)

DISCUSSION

The quantification of HCV viral load is essential for selecting an appropriate antiviral strategy and for monitoring the efficacy of treatment. Since HCV is known to be highly variable and rapidly

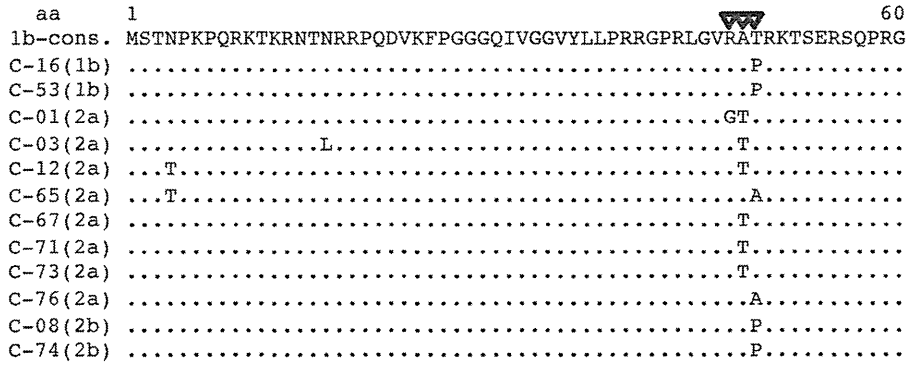

FIG 4 Alignment of the first 60 amino acids of the HCV core region of strains with polymorphisms at amino acid residues 47 to 49. The position numbers are given at the top. Dots indicate identical amino acids. The consensus sequence of 1b strains (1b cons.) isolated in this study was determined and used as a reference sequence. Genotypes of strains are given in parentheses. Positions of polymorphisms are indicated by inverted triangles above the sequence alignment.

evolving (23, 26), the assays for quantifying this virus should be unaffected by sequence polymorphisms. In this study, we established a reference panel with HCV-positive samples and evaluated the correlation among multiple assays for HCV RNA and core Ag quantification.

Using this reference panel, we found that the results from two HCV RNA assay kits, CAP/CTM-RNA and ART-RNA, correlated with excellent agreement ($r = 0.978$, $P < 0.0001$ [Fig. 1]), although discrepancies for values generated by these two assays have been reported for strains of genotypes 1, 2, and 4 (5, 6, 34). In Japan, the prevalent genotypes are 1b, 2a, and 2b (11); no genotype 4 sample was included in our reference panel (Table 1). In quantification with CAP/CTM-RNA, underestimation of HCV RNA titer has been reported for French genotype 2 samples (5). In our panel, no underestimation was observed for data from genotype 2 samples compared to values obtained using ART-RNA. Therefore, underestimation in quantification with CAP/CTM-RNA is expected to be rare in Japanese samples, and the two assays for HCV RNA quantification should be considered accurate and reliable, at least for Japanese samples. Additionally, the prepared reference panel appears to be suitable for the evaluation of HCV quantification assays, because genotypes of samples in this panel are representative of those found in Japan and viral loads are distributed evenly across the range of expected titers.

The quantification of HCV core Ag is an alternative test for HCV infection and viral load. However, in this study, several core Ag quantitative assays failed to provide accurate results for all of the samples in the reference panel (Fig. 2). Some quantified values were below the kits' detection limits. This shortcoming was mainly attributable to the lower sensitivity of the core Ag assay kits; increased sensitivity is urged in the future development of HCV core Ag kits. Among the kits tested here, Architect-Ag assay exhibited the highest sensitivity and was sufficient for quantifying the viral load in all samples. However, even in the case of Architect-Ag, theoretical lower limits of detection, calculated by correlation formula using CAP/CTM-RNA and ART-RNA, were 3.2 and 3.4 log IU/ml, respectively; these detection limits still exceeded the lower limits of the HCV RNA quantification assays. Therefore, the sensitivity of the available HCV core Ag assays is still insufficient to detect low-titer HCV infections. Core Ag kits therefore may be unsuitable for the detection of breakthrough hepatitis during antiviral therapy or for the detection of HCV infection in a window period.

Comparison between HCV RNA and core Ag assays revealed good correlations, with r coefficients ranging from 0.8877 to 0.9666 and P values being less than 0.0001 (Fig. 2; also, see Fig. S1 in the supplemental material). Therefore, the HCV core Ag levels may serve as an alternative to HCV RNA levels when titers remain within the detection ranges of the core Ag kits. However, several discordances were detected when core Ag levels were compared with those of HCV RNA. For one sample in our panel (sample C-01), core Ag levels were lower than expected when quantified using any of the three core Ag kits (Architect-Ag, Lumipulse-Ag, and Lumispot-Ag) (Fig. 3; also, see Fig. S2 in the supplemental material). Another sample (C-73) also yielded lower-than-expected levels when assayed with Architect-Ag and Lumipulse-Ag kits. Sequence analysis of the core region revealed that polymorphisms at aa 47 and 48 correlated with these underestimates by core Ag kits (see Fig. S4 in the supplemental material). These results are consistent with our previous study, which suggested that core Ag levels of HCV strain JFH-1 were underestimated by the Lumipulse-Ag kit in comparison to the ELISA-Ag assay (28). Strain JFH-1 harbors an Ala-to-Thr substitution at aa 48; conversion of Thr to Ala at this position in JFH-1 was sufficient to overcome this underestimation. This region of the core Ag presumably corresponds to one of the epitopes recognized by the monoclonal antibodies used in the Lumipulse-Ag kit, such that polymorphisms at this position affected the antigenicity of the core protein. In this study, we found that the presence of other polymorphisms in this region (aa 47 to 49) correlated with reduced core Ag levels as detected by Lumipulse-Ag, as well as by other assays (Architect-Ag and Lumispot-Ag). Sample C-01 demonstrated a drastic deviation from expected core Ag levels in these assays (Fig. 3; also, see Fig. S2 in the supplemental material). The HCV strain in this sample contains two polymorphisms (Arg to Gly at aa 47 and Ala to Thr at aa 48); the multiple polymorphisms may impair antibody binding more severely and therefore result in underestimation of core Ag levels. Interestingly, this sample exhibited reasonable core Ag levels when assayed using ELISA-Ag. Thus, the underestimation of core protein levels in this sample was kit dependent, suggesting the targeting of distinct epitopes by the antibodies used in each of these kits. This hypothesis could not be confirmed, because the identity of the epitopes targeted by each kit is proprietary.

Of 12 samples with amino acid polymorphisms in this region, 2 (5.7%) were of genotype 1b, 8 (30.8%) were of genotype 2a, and

TABLE 2 Number of strains in the sequence database[a] with polymorphisms at amino acid residues 47 to 49 of the HCV core region

Genotype	No. (%) of strains				
	Tested	With polymorphism			
		At aa 47 (R/C, G)	At aa 48 (A/T, P)	At aa 49 (T/A, P, L)	Total
1b	543	2 (0.36)	4 (0.74)	16 (2.96)	22 (4.1)
2a	24	0	6 (25.0)	1 (4.2)	7 (29.2)
2b	39	0	0	2 (6.9)	2 (6.9)

[a] http://s2as02.genes.nig.ac.jp/.

2 (11.8%) were of genotype 2b (Table 1). Searches of the Hepatitis Virus Database (http://s2as02.genes.nig.ac.jp/) revealed that corresponding amino acid polymorphisms were observed in 22 of 543 strains (4.1%) of genotype 1b, 7 of 24 strains (29.2%) of genotype 2a, and 2 of 39 strains (6.9%) of genotype 2b (Table 2). These percentages were consistent with our observations in the proposed reference panel. These data (our results and those from the database) clearly indicate that genotype 2a strains are the most frequent source of underestimation of core Ag levels. Notably, our search of the sequence database did not yield any HCV strain with multiple polymorphisms in the region from aa 47 to 49, as we saw in our sample C-01. Therefore, strains with such multiple polymorphisms are rare so far, but detection of this isolate among donated blood specimens suggests that such HCV strains could be emerging in clinical samples. For patients harboring such strains, HCV viral load may be underestimated if measurement of HCV viral load is performed by core Ag assay. Such underestimates may result in erroneous selection of therapy, adversely affecting patient outcome. Thus, this shortcoming in HCV core Ag assay kits needs to be addressed.

There is a growing need for evaluation of clinical assay kits with domestic specimen reference panels, since the performance of these kits may be affected by the genotypes or polymorphisms of predominant strains in different geographic regions. To our knowledge, such an investigation of HCV clinical assay kits with domestic specimens has not previously been conducted in Japan. The Japanese HCV reference panel described here was generated with plasma samples collected from Japanese volunteers. Each sample was divided into small aliquots, and the panel was prepared in multiple sets. The samples in our HCV reference panel represent the predominant strains and genotypes seen in Japan. We expect that this reference panel will be of use for the development, evaluation, and optimization of HCV assay kits for the Japanese clinical market.

In conclusion, we have established a Japanese reference panel for evaluation of HCV quantification assays. Using this reference panel, we found that two assay kits for HCV RNA could quantify HCV titers concordantly. We also found that the data generated by HCV core Ag assay kits correlated with the results of HCV RNA assays. However, the nominal core Ag levels measured by several kits underestimated actual levels for HCV samples with polymorphisms at aa 47 to 49 of the core Ag. The panel established in this study is expected to be useful for estimating the accuracy of currently available and upcoming HCV assay kits; such quality control is essential for clinical usage of these kits.

ACKNOWLEDGMENTS

This work was performed as part of a project for the preparation of reference panels of infectious disease specimens at the National Institute of Infectious Diseases in Japan. This work was also partly supported by grants-in-aid from the Japan Society for the Promotion of Science; the Ministry of Health, Labor and Welfare of Japan; the Ministry of Education, Culture, Sports, Science and Technology; and the Research on Health Sciences Focusing on Drug Innovation from the Japan Health Sciences Foundation.

We are grateful to Shun-ya Momose, Shigeharu Uchida, and Satoru Hino (Blood Service Headquarters, Japanese Red Cross Society) for providing specimens, to Tetsuro Suzuki (Department of Infectious Diseases, Hamamatsu University School of Medicine) for contribution to establish the reference panel, and to Kazuo Kobayashi and Masashi Tatsumi (the Committee of the Reference Panels of Infectious Disease Specimens at the National Institute of Infectious Diseases in Japan) for their helpful suggestions. We also thank the manufacturers of HCV quantification kits, including Roche Diagnostics (Tokyo, Japan), Abbott Japan (Tokyo, Japan), Fujirebio (Tokyo, Japan), Eiken Chemical (Tokyo, Japan), and Ortho Clinical Diagnostics (Tokyo, Japan), for quantification of reference panel samples.

REFERENCES

1. **Alvarez M, Planelles D, Vila E, Montoro J, Franco E.** 2004. Prolonged hepatitis C virus seroconversion in a blood donor, detected by HCV antigen test in parallel with HCV RNA. Vox Sang. **86**:266–267.
2. **Aoyagi K, et al.** 1999. Development of a simple and highly sensitive enzyme immunoassay for hepatitis C virus core antigen. J. Clin. Microbiol. **37**:1802–1808.
3. **Aoyagi K, et al.** 2001. Performance of a conventional enzyme immunoassay for hepatitis C virus core antigen in the early phases of hepatitis C infection. Clin. Lab. **47**:119–127.
4. **Bossler A, et al.** 2011. Performance of the COBAS(R) AmpliPrep/COBAS TaqMan(R) automated system for hepatitis C virus (HCV) quantification in a multi-center comparison. J. Clin. Virol. **50**:100–103.
5. **Chevaliez S, Bouvier-Alias M, Brillet R, Pawlotsky JM.** 2007. Overestimation and underestimation of hepatitis C virus RNA levels in a widely used real-time polymerase chain reaction-based method. Hepatology **46**: 22–31.
6. **Elkady A, et al.** 2010. Performance of two real-time RT-PCR assays for quantitation of hepatitis C virus RNA: evaluation on HCV genotypes 1–4. J. Med. Virol. **82**:1878–1888.
7. **Enomoto M, et al.** 2005. Chemiluminescence enzyme immunoassay for monitoring hepatitis C virus core protein during interferon-alpha2b and ribavirin therapy in patients with genotype 1 and high viral loads. J. Med. Virol. **77**:77–82.
8. **Feld JJ, Hoofnagle JH.** 2005. Mechanism of action of interferon and ribavirin in treatment of hepatitis C. Nature **436**:967–972.
9. **Feld JJ, Liang TJ.** 2006. Hepatitis C—identifying patients with progressive liver injury. Hepatology **43**:S194–S206.
10. **Icardi G, et al.** 2001. Novel approach to reduce the hepatitis C virus (HCV) window period: clinical evaluation of a new enzyme-linked immunosorbent assay for HCV core antigen. J. Clin. Microbiol. **39**:3110–3114.
11. **Ikeda K, et al.** 1996. Hepatitis C virus subtype 3b infection in a hospital in Japan: epidemiological study. J. Gastroenterol. **31**:801–805.
12. **Kaiser T, et al.** 2008. Kinetics of hepatitis C viral RNA and HCV-antigen during dialysis sessions: evidence for differential viral load reduction on dialysis. J. Med. Virol. **80**:1195–1201.
13. **Leary TP, et al.** 2006. A chemiluminescent, magnetic particle-based immunoassay for the detection of hepatitis C virus core antigen in human serum or plasma. J. Med. Virol. **78**:1436–1440.
14. **Liang TJ.** 1998. Combination therapy for hepatitis C infection. N. Engl. J. Med. **339**:1549–1550.
15. **Liang TJ, Rehermann B, Seeff LB, Hoofnagle JH.** 2000. Pathogenesis, natural history, treatment, and prevention of hepatitis C. Ann. Intern. Med. **132**:296–305.
16. **Matsuura K, et al.** 2009. Abbott RealTime hepatitis C virus (HCV) and Roche Cobas AmpliPrep/Cobas TaqMan HCV assays for prediction of sustained virological response to pegylated interferon and ribavirin in chronic hepatitis C patients. J. Clin. Microbiol. **47**:385–389.

17. **Mederacke I, et al.** 2009. Performance and clinical utility of a novel fully automated quantitative HCV-core antigen assay. J. Clin. Virol. **46**:210–215.
18. **Medici MC, et al.** 2011. *Hepatitis C virus core antigen: analytical performances, correlation with viremia and potential applications of a quantitative, automated immunoassay.* J. Clin. Virol. **51**:264–269.
19. **Miedouge M, et al.** 2010. Analytical evaluation of HCV core antigen and interest for HCV screening in haemodialysis patients. J. Clin. Virol. **48**: 18–21.
20. **Morota K, et al.** 2009. A new sensitive and automated chemiluminescent microparticle immunoassay for quantitative determination of hepatitis C virus core antigen. J. Virol. Methods **157**:8–14.
21. **Moscato GA, et al.** 2011. Quantitative determination of hepatitis C core antigen in therapy monitoring for chronic hepatitis C. Intervirology **54**: 61–65.
22. **Nubling CM, Unger G, Chudy M, Raia S, Lower J.** 2002. Sensitivity of HCV core antigen and HCV RNA detection in the early infection phase. Transfusion **42**:1037–1045.
23. **Ogata N, Alter HJ, Miller RH, Purcell RH.** 1991. Nucleotide sequence and mutation rate of the H strain of hepatitis C virus. Proc. Natl. Acad. Sci. U. S. A. **88**:3392–3396.
24. **Park Y, Lee JH, Kim BS, Kim DY, Han KH, Kim HS.** 2010. New automated hepatitis C virus (HCV) core antigen assay as an alternative to real-time PCR for HCV RNA quantification. J. Clin. Microbiol. **48**:2253–2256.
25. **Pawlotsky JM.** 2006. Therapy of hepatitis C: from empiricism to eradication. Hepatology **43**:S207–S220.
26. **Robertson B, et al.** 1998. Classification, nomenclature, and database development for hepatitis C virus (HCV) and related viruses: proposals for standardization. Arch. Virol. **143**:2493–2503.
27. **Ross RS, et al.** 2010. Analytical performance characteristics and clinical utility of a novel assay for total hepatitis C virus core antigen quantification. J. Clin. Microbiol. **48**:1161–1168.
28. **Saeed M, et al.** 2009. *Evaluation of hepatitis C virus core antigen assays in detecting recombinant viral antigens of various genotypes.* J. Clin. Microbiol. **47**:4141–4143.
29. **Seeff LB, Hoofnagle JH.** 2002. National Institutes of Health Consensus Development Conference: management of hepatitis C: 2002. Hepatology **36**:S1–S2.
30. **Takahashi M, Saito H, Higashimoto M, Atsukawa K, Ishii H.** 2005. Benefit of hepatitis C virus core antigen assay in prediction of therapeutic response to interferon and ribavirin combination therapy. J. Clin. Microbiol. **43**:186–191.
31. **Tanaka E, et al.** 2000. Evaluation of a new enzyme immunoassay for hepatitis C virus (HCV) core antigen with clinical sensitivity approximating that of genomic amplification of HCV RNA. Hepatology **32**:388–393.
32. **Tanaka Y, et al.** 2003. High stability of enzyme immunoassay for hepatitis C virus core antigen-evaluation before and after incubation at room temperature. Hepatol. Res. **26**:261–267.
33. **Vermehren J, et al.** 2008. Differences between two real-time PCR-based hepatitis C virus (HCV) assays (RealTime HCV and Cobas AmpliPrep/Cobas TaqMan) and one signal amplification assay (Versant HCV RNA 3.0) for RNA detection and quantification. J. Clin. Microbiol. **46**:3880–3891.
34. **Vermehren J, et al.** 2011. Development of a second version of the Cobas AmpliPrep/Cobas TaqMan hepatitis C virus quantitative test with improved genotype inclusivity. J. Clin. Microbiol. **49**:3309–3315.
35. **Vermehren J, et al.** 2011. Multi-center evaluation of the Abbott RealTime HCV assay for monitoring patients undergoing antiviral therapy for chronic hepatitis C. J. Clin. Virol. **52**:133–137.

SUPPLEMENTALY MATERIALS

SUPPLEMENTARY FIGURE LEGEND

Supplementary Figure 1.

Correlation between ART-RNA and core Ag levels as quantified by five commercial kits. Data for core Ag levels were converted to log fmol/L prior to analysis. In each plot, the lower limit of detection of the respective core Ag assay is indicated by a dotted line, and the respective correlation coefficient and formula are provided at the top of each plot. Data for samples below the lower detection limit of each assay are indicated by shaded (gray) circles, and sample designations are indicated by arrows.

Supplementary Figure 2.

Bland-Altman plot analysis of ART-RNA and core Ag levels as quantified by five commercial kits. These plots show the difference between the

values of HCV RNA and core Ag as a function of the average of these two values. Data for core Ag levels were converted to log fmol/L prior to analysis. The bias and 95% limits of agreements are indicated by bold and dashed lines, respectively. Data for samples with polymorphisms at amino acid residues 47 – 49 are indicated by closed (black) circles. Sample designations for samples outside the 95% limits are indicated by arrows.

Supplementary Figure 3.

The phylogenetic tree constructed with sequences determined in this study. This phylogenetic tree contains 80 strains in the reference panel, reference strains submitted from Japan (24 strains of genotype 1b, 19 strains of genotype 2a, and 25 strains of genotype 2b), and 7 representative strains of each genotype (H77; genotype 1a, Con1, BK, and Taiwan; genotype 1b, BEBE1; genotype 2c, K3a; genotype 3a, and ED43; genotype 4a). The genetic distances were calculated by 6-parameter method, and a phylogenetic tree was constructed by neighbor-joining method by use of software in Hepatitis Virus

Database (http://s2as02.genes.nig.ac.jp/). The length of horizontal bars indicates the numbers of nucleotide substitutions per site.

Supplementary Figure 4.

Alignment of deduced amino acids in the HCV core region. The position number of the amino acids is indicated at both ends of each sequence. Dots indicate identical amino acids. The consensus sequence of 1b strains (1b cons.) isolated in this study was determined and used as a reference sequence. Genotypes of strains in alignment are indicated in parentheses. Strains with discordance in multiple core Ag assays as compared with both RNA quantitative assays are indicated in bold lettering (C-01 and C-73).

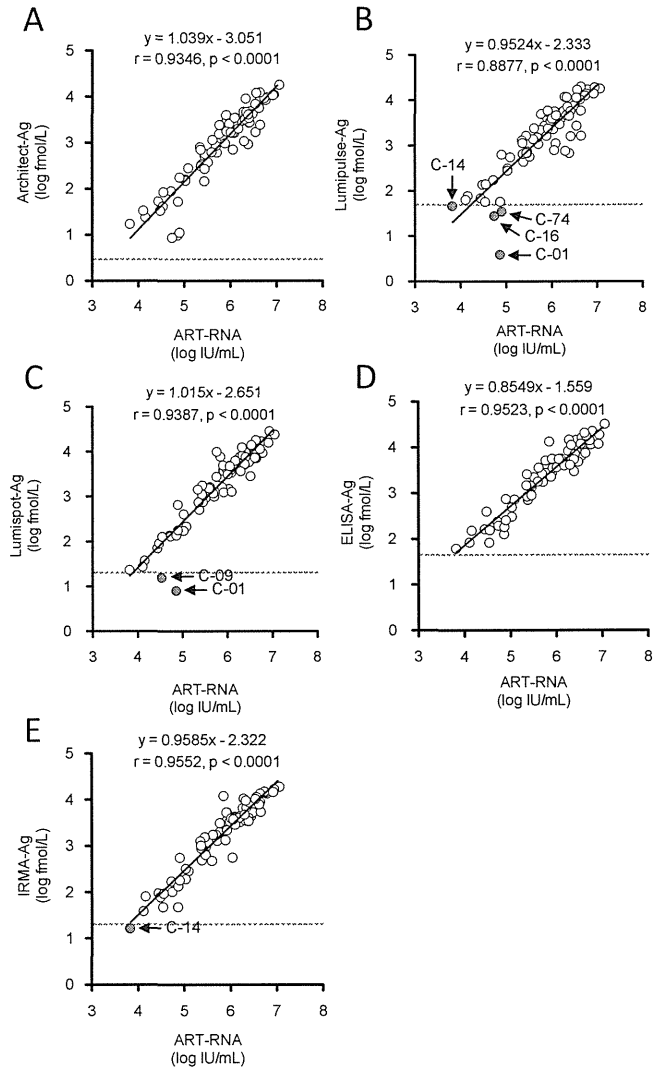

Supplementary Figure 1

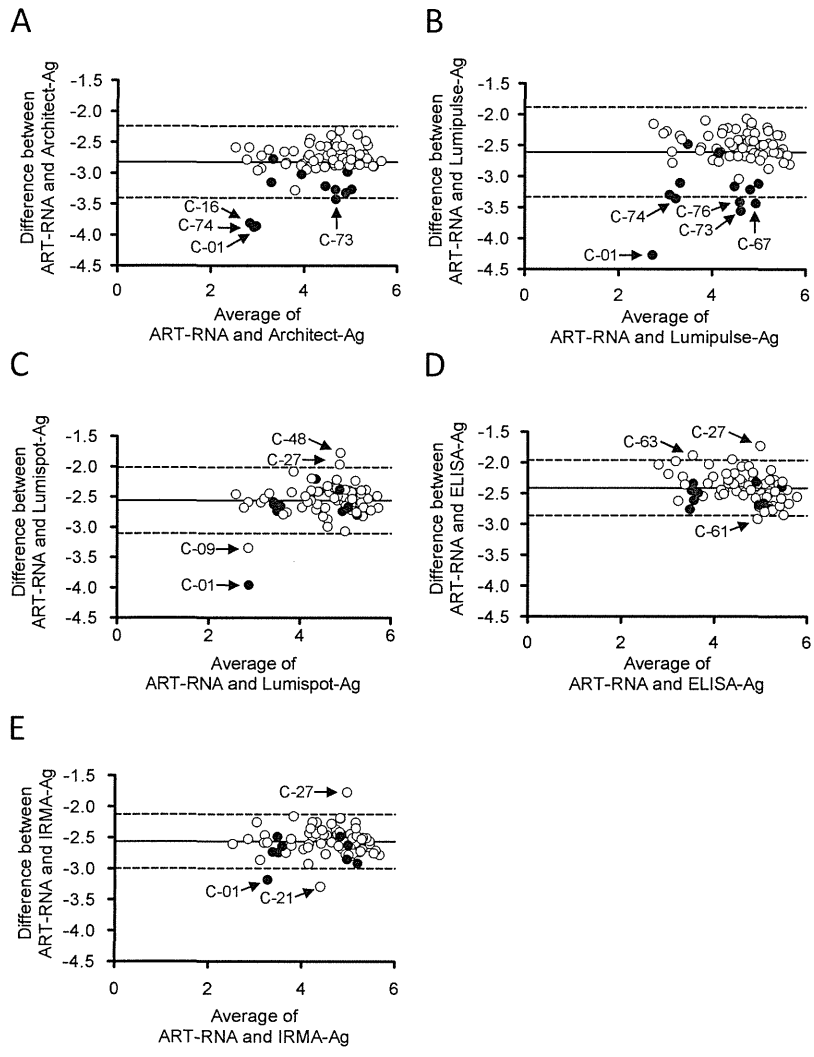

Supplementary Figure 2

Supplementary Figure 3

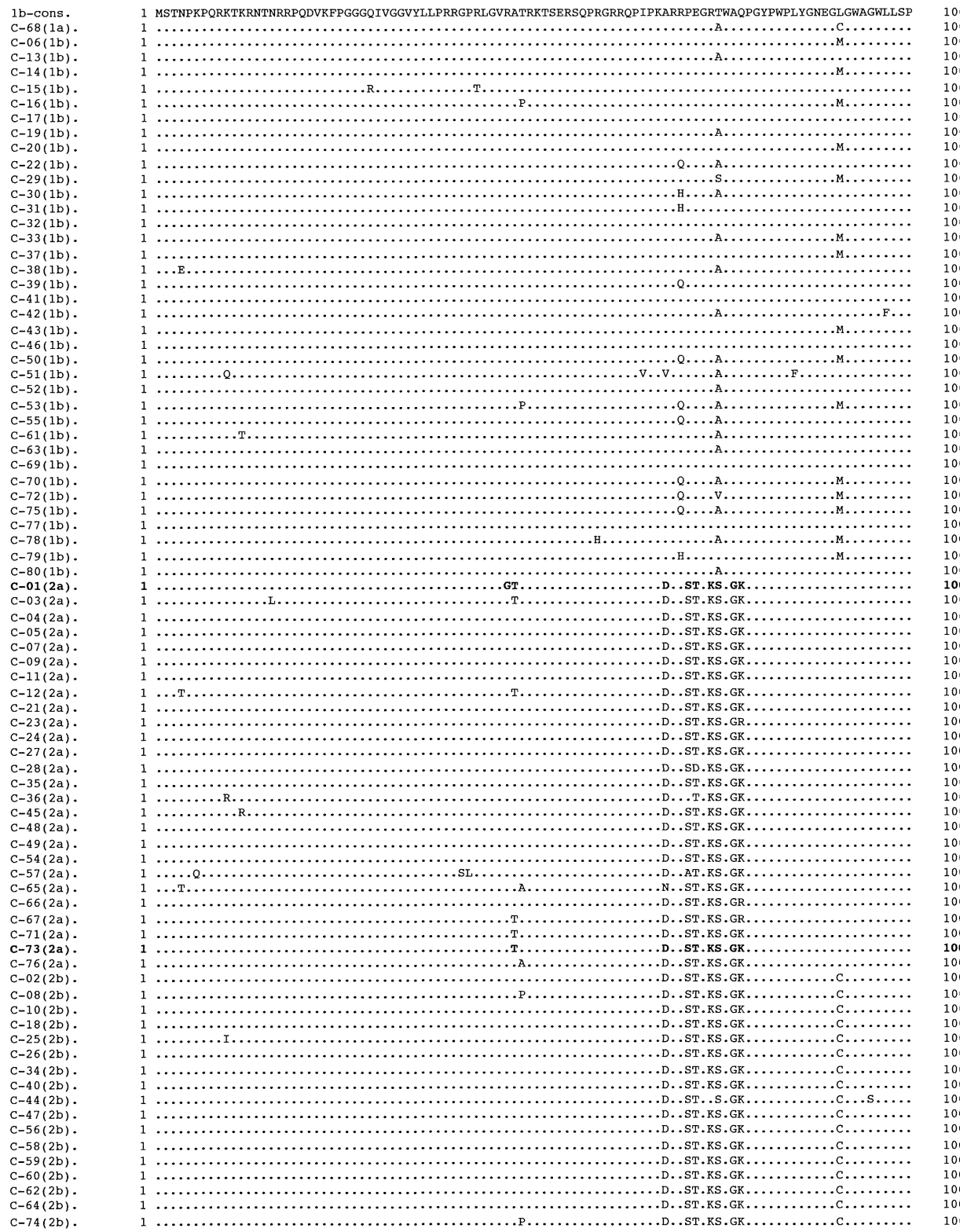

Supplementary Figure 4

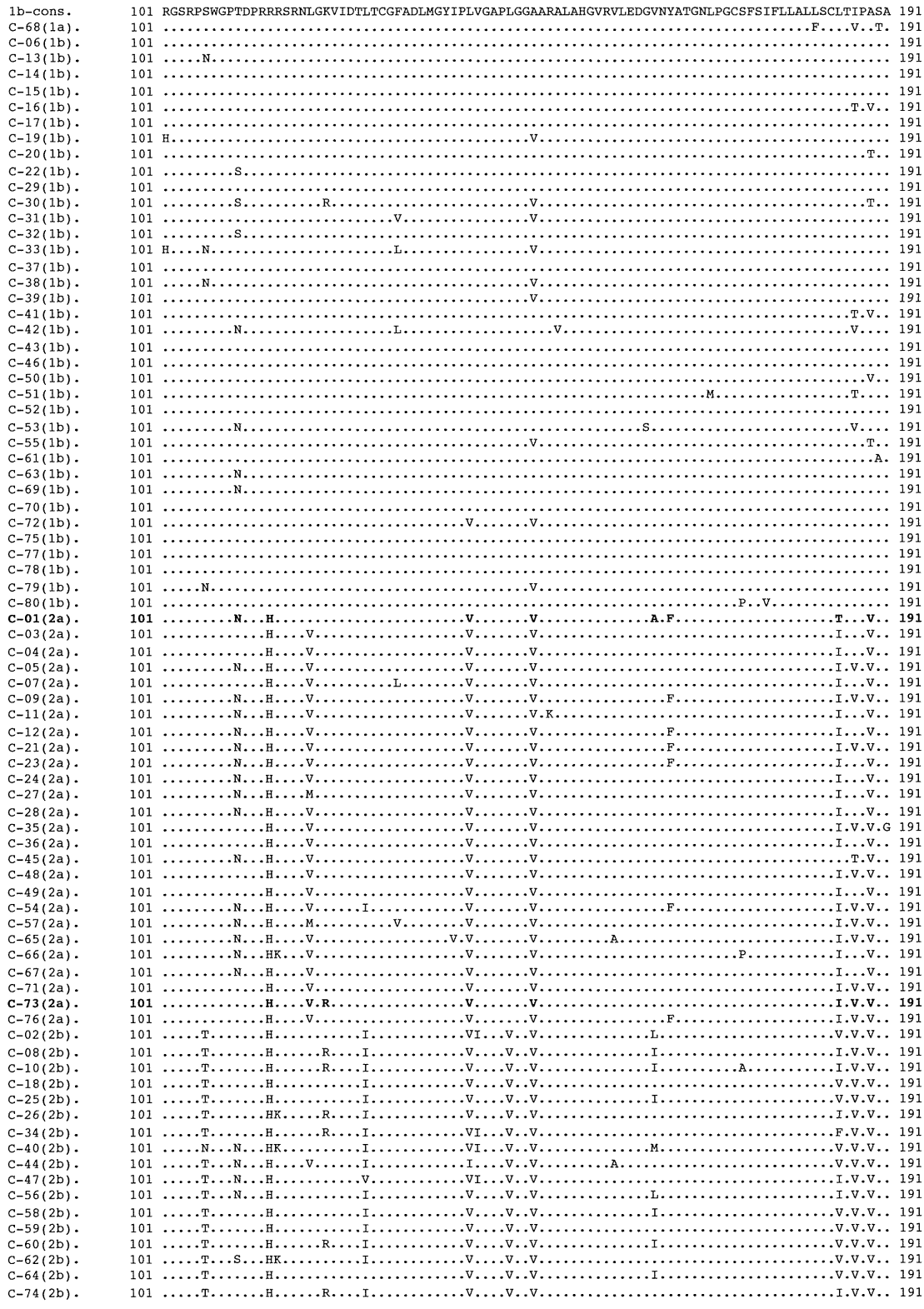

Supplementary Figure 4
Continued

JVI
Journals.ASM.org

Production of Infectious Chimeric Hepatitis C Virus Genotype 2b Harboring Minimal Regions of JFH-1

Asako Murayama,[a] Takanobu Kato,[a] Daisuke Akazawa,[a] Nao Sugiyama,[a] Tomoko Date,[a] Takahiro Masaki,[a] Shingo Nakamoto,[b] Yasuhito Tanaka,[c] Masashi Mizokami,[d] Osamu Yokosuka,[b] Akio Nomoto,[e]* and Takaji Wakita[a]

Department of Virology II, National Institute of Infectious Diseases, Shinjuku-ku, Tokyo, Japan[a]; Department of Medicine and Clinical Oncology, Graduate School of Medicine, Chiba University, Chuo, Chiba, Japan[b]; Department of Virology and Liver Unit, Nagoya City University Graduate School of Medical Sciences, Kawasumi, Mizuho, Nagoya, Japan[c]; The Research Center for Hepatitis and Immunology, National Center for Global Health and Medicine, Ichikawa, Chiba, Japan[d]; and Department of Microbiology, Graduate School of Medicine, University of Tokyo, Bunkyo-ku, Tokyo, Japan[e]

To establish a cell culture system for chimeric hepatitis C virus (HCV) genotype 2b, we prepared a chimeric construct harboring the 5′ untranslated region (UTR) to the E2 region of the MA strain (genotype 2b) and the region of p7 to the 3′ UTR of the JFH-1 strain (genotype 2a). This chimeric RNA (MA/JFH-1.1) replicated and produced infectious virus in Huh7.5.1 cells. Replacement of the 5′ UTR of this chimera with that from JFH-1 (MA/JFH-1.2) enhanced virus production, but infectivity remained low. In a long-term follow-up study, we identified a cell culture-adaptive mutation in the core region (R167G) and found that it enhanced virus assembly. We previously reported that the NS3 helicase (N3H) and the region of NS5B to 3′ X (N5BX) of JFH-1 enabled replication of the J6CF strain (genotype 2a), which could not replicate in cells. To reduce JFH-1 content in MA/JFH-1.2, we produced a chimeric viral genome for MA harboring the N3H and N5BX regions of JFH-1, combined with a JFH-1 5′ UTR replacement and the R167G mutation (MA/N3H+N5BX-JFH1/R167G). This chimeric RNA replicated efficiently, but virus production was low. After the introduction of four additional cell culture-adaptive mutations, MA/N3H+N5BX-JFH1/5am produced infectious virus efficiently. Using this chimeric virus harboring minimal regions of JFH-1, we analyzed interferon sensitivity and found that this chimeric virus was more sensitive to interferon than JFH-1 and another chimeric virus containing more regions from JFH-1 (MA/JFH-1.2/R167G). In conclusion, we established an HCV genotype 2b cell culture system using a chimeric genome harboring minimal regions of JFH-1. This cell culture system may be useful for characterizing genotype 2b viruses and developing antiviral strategies.

Hepatitis C virus (HCV) is a major cause of chronic liver disease (5, 13), but the lack of a robust cell culture system to produce virus particles has hampered the progress of HCV research (2). Although the development of a subgenomic replicon system has enabled research into HCV RNA replication (15), infectious virus particle production has not been possible. Recently, an HCV cell culture system was developed using a genotype 2a strain, JFH-1, cloned from a fulminant hepatitis patient (14, 29, 32), thereby allowing investigation of the entire life cycle of this virus. However, several groups of investigators have reported genotype- and/or strain-dependent effects of some antiviral reagents (6, 17) and neutralizing antibodies (7, 25). Therefore, efficient virus production systems using various genotypes and strains are indispensable for HCV research and the development of antiviral strategies.

The JFH-1 strain is the first HCV strain that can efficiently produce HCV particles in HuH-7 cells (29). Other strains can replicate and produce infectious virus by HCV RNA transfection, but the efficiency is far lower than that of JFH-1 (24, 31). In the case of replication-incompetent strains, chimeric virus containing the JFH-1 nonstructural protein coding region is useful for analyses of viral characteristics (6, 9, 14, 23, 30, 31).

In this study, we developed a genotype 2b chimeric infectious virus production system using the MA strain (accession number AB030907) (19) harboring minimal regions of JFH-1 and cell culture-adaptive mutations that enhance infectious virus production.

MATERIALS AND METHODS

Cell culture. Huh7.5.1 cells (a kind gift from Francis V. Chisari) (32) and Huh7-25 cells (1) were cultured at 37°C in Dulbecco's modified Eagle's medium containing 10% fetal bovine serum under 5% CO_2 conditions. For follow-up study, RNA-transfected cells were passaged every 2 to 5 days depending on cell status.

Full-length genomic HCV constructs. Plasmids used in the analysis of genomic RNA replication were constructed based on pJFH1 (29) and pMA (19). For convenience, an EcoRI recognition site was introduced upstream of the T7 promoter region of pMA by PCR, and an XbaI recognition site was introduced at the end of the 3′ untranslated region (UTR). To construct MA/JFH-1, the EcoRI-BsaBI (nucleotides [nt] 1 to 2570; 5′ UTR to E2) fragment of pMA was substituted into pJFH1 (Fig. 1A). Replacement of the 5′ UTR was performed by exchanging the EcoRI-AgeI (nt 1 to 159) fragment. A point mutation in the core region (R167G) was introduced into MA chimeric constructs by PCR using the following primers: sense, 5′-TTA TGC AAC GGG GAA TTT ACC CGG TTG CTC T-3′; antisense, 5′-GGT AAA TTC CCC GTT GCA TAA TTT ATC CCG TC-3′. G167R substitution in the JFH-1 construct was performed by PCR using the following primers: sense, 5′-ATT ATG CAA CAA GGA ACC TAC CCG GTT TCC C-3′; antisense, 5′-GGT AGG TTC CTT GTT GCA TAA TTA ACC CCG TC-3′. Point mutations (L814S, R1012G, T1106A, and V1951A) were introduced into MA chimeric constructs by PCR using the following primers: L814S, 5′-GCT TAC GCC TCG GAC GCC GCT GAA CAA GGG G-3′ (sense) and 5′-AGC GGC GTC CGA GGC GTA AGC CTG CTG CGG C-3′ (antisense); R1012G, 5′-GAG GCT AGG TGG

Received 13 June 2011 Accepted 23 November 2011
Published ahead of print 7 December 2011
Address correspondence to Takaji Wakita, wakita@nih.go.jp.
* Present address: Institute of Microbial Chemistry, Shinagawa-ku, Tokyo, Japan.

doi:10.1128/JVI.05386-11

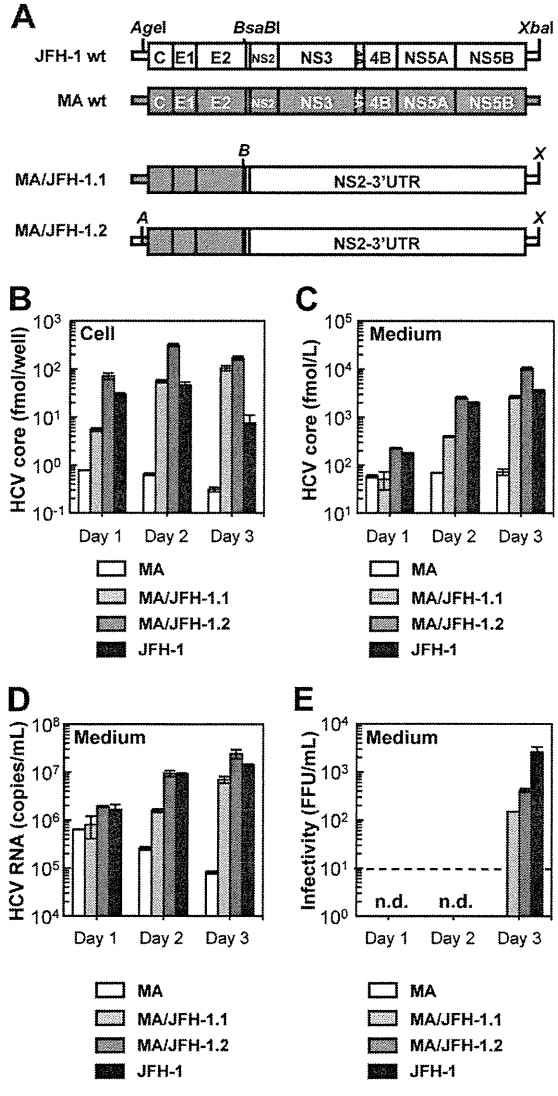

FIG 1 Replication and virus production by MA/JFH-1 chimeras in Huh7.5.1 cells. (A) Schematic structures of JFH-1, MA, and two MA/JFH-1 chimeras (MA/JFH-1.1 and MA/JFH-1.2). The junction of JFH-1 and MA in the 5′ UTR is an AgeI site, and the junction of MA and JFH-1 in the NS2 region is a BsaBI site. A, AgeI; B, BsaBI; X, XbaI. (B to E) Chimeric HCV RNA replication in Huh7.5.1 cells. HCV core protein level in cells (B) and culture medium (C) and HCV RNA levels in medium (D) and infectivity of culture medium (E) from HCV RNA-transfected Huh7.5.1 cells are shown. Ten micrograms of HCV RNA was transfected into Huh7.5.1 cells, and cells and culture medium were harvested on days 1, 2, and 3. n.d., not determined. Assays were performed three times independently, and data are presented as means ± standard deviation. Dashed line indicates detection limit. wt, wild type.

GGA AGT TCT GCT CGG CCC T-3′ (sense) and 5′-AGA ACT TCC CCA CCT AGC CTC GCG GAA ACC G-3′ (antisense); T1106A, 5′-CAG ATG TAC GCC AGC GCA GAG GGG GAC CTC-3′ (sense) and 5′-CTG CGC TGG CGT ACA TCT GGG TGA CTG GTC-3′ (antisense); and V1951A, 5′-GTG ACG CAG GCG TTA AGC TCA CTC ACA ATT ACC-3′ (sense) and 5′-TGA GCT TAA CGC CTG CGT CAC GCG CAG CGA G-3′ (antisense). To construct the MA chimeric virus harboring minimal regions of JFH-1 (MA/N3H+N5BX-JFH1), ClaI (nt 3930), EcoT22I (nt 5294), and BsrGI (nt 7782) recognition sites were introduced into pMA by site-directed mutagenesis. The 5′ UTR (EcoRI-AgeI), the region of the NS3 helicase (N3H; ClaI-EcoT22I), and the region of NS5B to 3′ X (N5BX; BsrGI-XbaI) were then replaced with the corresponding regions from JFH-1.

RNA synthesis, transfection, and determination of infectivity. RNA synthesis and transfection were performed as described previously (12, 22). Determination of infectivity was also performed as described previously, with infectivity expressed as the number of focus-forming units per milliliter (FFU/ml) (12, 22). When necessary, culture medium was concentrated 20-fold in Amicon Ultra-15 spin columns (100-kDa molecular-weight-cutoff; Millipore, Bedford, MA) in order to determine infectivity.

Quantification of HCV core protein and HCV RNA. In order to estimate the concentration of HCV core protein in culture medium, we performed a chemiluminescence enzyme immunoassay (Lumipulse II HCV core assay; Fujirebio, Tokyo, Japan) in accordance with the manufacturer's instructions. HCV RNA from harvested cells or culture medium was isolated using an RNeasy Mini RNA kit (Qiagen, Tokyo, Japan) or QiaAmp Viral RNA Minikit (Qiagen), respectively. Copy number of HCV RNA was determined by real-time quantitative reverse transcription-PCR (qRT-PCR), as described previously (28).

HCV sequencing. Total RNA in culture supernatant was extracted with Isogen-LS (Nippon Gene Co., Ltd., Tokyo, Japan). cDNA was synthesized using Superscript III Reverse Transcriptase (Invitrogen, Carlsbad, CA). cDNA was subsequently amplified with LA *Taq* DNA polymerase (TaKaRa, Shiga, Japan). Four separate PCR primer sets were used to amplify the fragments of nt 130 to 2909, 2558 to 5142, 4784 to 7279, and 7081 to 9634 covering the entire open reading frame and part of the 5′ UTR and 3′ UTR of the MA strain. Sequences of amplified fragments were determined directly.

Immunostaining. Infected cells were cultured on Multitest Slides (MP Biomedicals, Aurora, OH) and were fixed in acetone-methanol (1:1, vol/vol) for 15 min at −20°C. After a blocking step, infected cells were visualized with anti-core protein antibody (clone 2H9) (29) and Alexa Fluor 488 goat anti-mouse IgG (Invitrogen), and nuclei were visualized with 4′,6′-diamidino-2-phenylindole (DAPI).

Assessment of interferon sensitivity. Two micrograms of *in vitro* transcribed RNA was transfected into 3×10^6 Huh7.5.1 cells. Four hours after transfection, cells were placed in fresh medium or medium containing 0.1, 1, 10, 100, and 1,000 IU/ml of interferon α-2b (Intron A; Schering-Plough Corporation, Osaka, Japan). Culture medium was then harvested on day 3, and HCV core levels in the cells and in the medium were measured.

Statistical analysis. Significant differences were evaluated by Student's *t* test. A *P* value of <0.05 was considered significant.

RESULTS

Transient replication and production of 2b/2a chimeric virus. We first tested whether the MA strain (genotype 2b) (19) was able to replicate and produce infectious virus in cultured cells. When the *in vitro* transcribed RNA of MA was transfected into Huh7.5.1 cells, a highly HCV-permissive cell line, replication and virus production were not observed (Fig. 1A to C). We then tested whether 2b/2a chimeric RNA harboring the structural region (5′ UTR to E2) of the MA strain and the nonstructural region (p7 to 3′ UTR) of JFH-1 (Fig. 1A, MA/JFH-1.1) was able to replicate in the cells. After MA/JFH-1.1 RNA transfection, time-dependent accumulation of core protein in the cells (Fig. 1B) and culture medium (Fig. 1C) was observed, indicating that MA/JFH-1.1 RNA was able to replicate in the cells autonomously. HCV RNA levels in the medium were determined by qRT-PCR, and time-dependent increases in HCV RNA level were also observed (Fig. 1D). Infectious virus production was observed on day 3, but infectivity was 17.6-fold lower than that of JFH-1 (Fig. 1E).

In order to improve the level of infectious virus production, we tested another chimeric construct, MA/JFH-1.2, which contained an additional MA-to-JFH-1 replacement of the 5′ UTR (Fig. 1A),

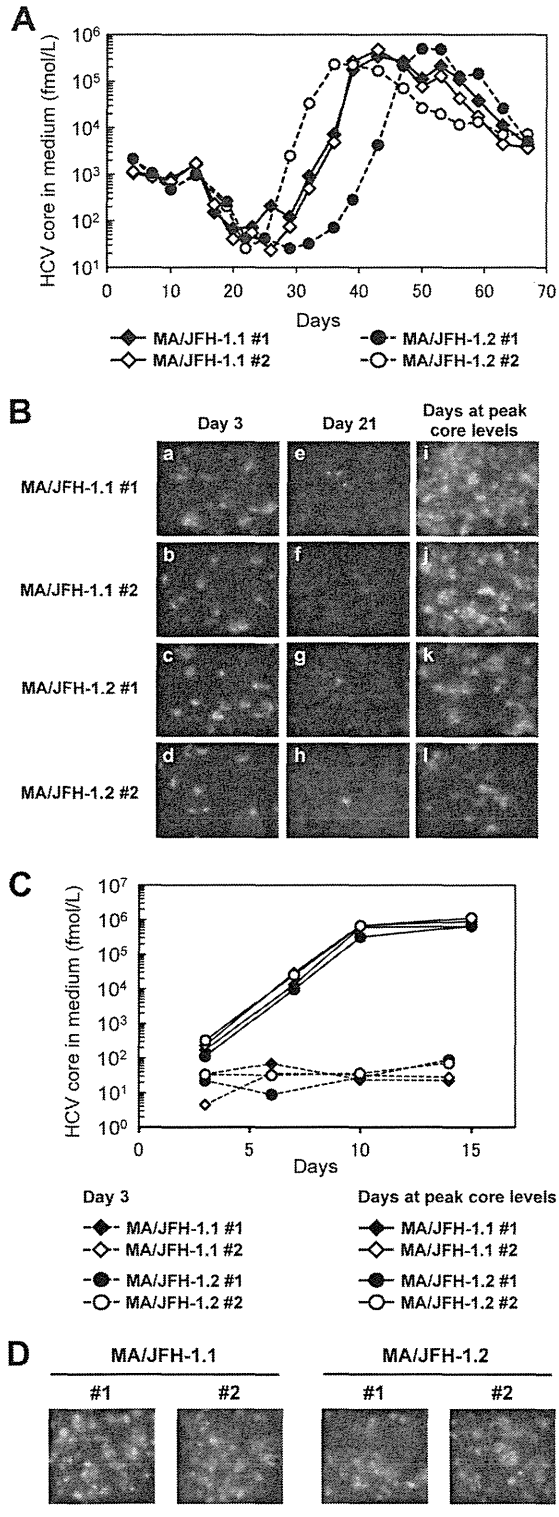

FIG 2 Long-term culture of MA/JFH-1.1 and MA/JFH-1.2 RNA-transfected cells. Ten micrograms of HCV RNA was transfected into Huh7.5.1 cells, and cells were passaged every 2 to 5 days, depending on cell status. Culture medium was collected after every passage, and HCV core protein levels were measured. Transfection was performed twice for each chimeric RNA (1 and 2 for each construct). (A) HCV core protein levels in culture medium from MA/JFH-1.1 and MA/JFH-1.2 RNA-transfected cells. (B) Immunostained cells at 3 days after transfection (a to d), at 21 days after transfection (e to h), and at the time of peak core levels (days 42 to 49). Infected cells were visualized with anti-core protein antibody (green), and nuclei were visualized with DAPI (blue). (C) Infection of naïve cells by culture medium at an MOI of 0.001. (D) Immunostained cells at 15 days after infection with medium at peak core protein levels (Fig. 2A) at an MOI of 0.001. Infected cells were visualized with anti-core antibody (green), and nuclei were visualized with DAPI (blue).

TABLE 1 HCV core protein levels and infectivity in culture medium immediately after RNA transfection (day 3) and after long-term culture (days 35 to 49)

Sample period and virus	Sample no.	Day no.[a]	HCV core (fmol/liter)	Infectivity (FFU/ml)
After transfection				
MA/JFH-1.1	1	3	1.06×10^3	5.00×10^1
	2	3	1.14×10^3	5.70×10^1
MA/JFH-1.2	1	3	2.14×10^3	7.30×10^1
	2	3	2.15×10^3	9.30×10^1
After long-term culture				
MA/JFH-1.1	1	42	3.38×10^5	1.62×10^5
	2	42	4.70×10^5	3.23×10^5
MA/JFH-1.2	1	35	2.27×10^5	1.61×10^5
	2	49	4.93×10^5	3.27×10^5

[a] For the long-term culture, the days are those of peak core protein levels.

as a 5′ UTR replacement from J6CF (genotype 2a) to JFH-1 enhanced virus production of chimeric J6CF virus harboring the region of NS2 to 3′ X of JFH-1 (J6/JFH-1) (A. Murayama et al., unpublished data). The core protein accumulation levels with MA/JFH-1.2 RNA-transfected cells were higher than those with MA/JFH-1.1 ($P < 0.05$) (Fig. 1B). Similarly, core protein and HCV RNA levels in the medium of MA/JFH-1.2 RNA-transfected cells were higher than those of MA/JFH-1.1 ($P < 0.05$) (Fig. 1C and D). Infectivity on day 3 was also higher than with MA/JFH-1.1 ($P < 0.05$) (Fig. 1E), indicating that the 5′ UTR of JFH-1 enhanced virus production. However, infectivity of medium from MA/JFH-1.2 RNA-transfected cells on day 3 remained 6.4-fold lower than that of JFH-1 although HCV RNA levels in the medium were similar to those of JFH-1 (Fig. 1D and E).

These results indicate that 2b/2a chimeric RNA is able to replicate autonomously in Huh7.5.1 cells and produce infectious virus although infectivity remains lower than that of JFH-1.

Assembly-enhancing mutation in core region introduced during long-term culture. Because MA/JFH-1.1 and MA/JFH-1.2 replicated efficiently but produced small amounts of infectious virus, we performed long-term culture of these RNA-transfected cells in order to examine whether these chimeric RNAs would continue replicating and producing infectious virus over the long term. We prepared two RNA-transfected cell lines for each construct (MA/JFH-1.1 and MA/JFH-1.2) as both of these replicated and produced infectious virus at different levels.

Immediately after transfection, core protein levels and infectivity in culture medium were low (1.06×10^3 to 2.15×10^3 fmol/liter and 5.00×10^1 to 9.30×10^1 FFU/ml, respectively) (Fig. 2A and Table 1) although a considerable number of core protein-positive cells were observed by immunostaining (Fig. 2B, frames a to d). Subsequently, core protein levels in the culture medium decreased gradually (Fig. 2A), and core protein-positive cells were rare (Fig. 2B, frames e to h). However, at 30 to 40 days

after transfection, core protein levels in the supernatants of all chimeric RNA-transfected cells increased and reached 2.27×10^5 to 4.93×10^5 fmol/liter (Fig. 2A and Table 1). Infectivity in the culture medium also increased (1.61×10^5 to 3.27×10^5 FFU/ml) (Table 1), and at this point, most of the cells were core protein positive (Fig. 2B, frame i to l).

As the infectivity of culture supernatant of MA/JFH-1 RNA-transfected cells appeared to increase after long-term culture, we compared viral spread by infection with these supernatants on day 3 (immediately after transfection) and for each peak in core protein levels (after long-term culture). When naïve Huh7.5.1 cells were infected with supernatant on days corresponding to a peak in core protein levels at a multiplicity of infection (MOI) of 0.001, core protein levels in the medium increased rapidly and reached 0.64×10^6 to 1.13×10^6 fmol/liter by day 15 after infection (Fig. 2C). Immunostained images showed that most cells were HCV core protein positive on day 15 (Fig. 2D). When naïve Huh7.5.1 cells were infected with supernatant from day 3 at an MOI of 0.001, core protein levels in the medium did not increase under these conditions (Fig. 2C). These results indicate that both MA/JFH-1 chimeric viruses (MA/JFH-1.1 and MA/JFH-1.2) acquired the ability to spread rapidly after long-term culture.

As the characteristics of the MA/JFH-1 virus changed in long-term culture, we analyzed the possible mutations in the viral genome from the supernatant at each peak in core protein levels (Table 1, days at peak core levels). Nine- to 12-nucleotide mutations were found in the viral genome from each supernatant, and the detected mutations were distributed along the entire genome. Among these mutations, a common nonsynonymous mutation was found in the core region (Arg to Gly at amino acid [aa]167, R167G).

In order to test the effects of R167G on virus production, an R167G substitution was introduced into MA/JFH-1.2 as MA/JFH-1.2 replicated and produced infectious virus more efficiently than MA/JFH-1.1. HCV core protein levels in cells and medium of MA/JFH-1.2 with R167G (MA/JFH-1.2/R167G) were higher than with MA/JFH-1.2 ($P < 0.05$) (Fig. 3A and B). HCV RNA levels in the medium of MA/JFH-1.2/R167G RNA-transfected cells were also higher than with MA/JFH-1.2 ($P < 0.05$) (Fig. 3C). Infectious virus production was also increased by the R167G mutation ($P < 0.05$) (Fig. 3D) and was 8.7-fold higher than that of JFH-1 RNA-transfected cells on day 3 ($P < 0.05$) (Fig. 3D).

We then tested whether R167G was responsible for the rapid spread observed in culture supernatant after long-term culture by monitoring virus spread after infection of naïve Huh7.5.1 with culture medium taken 3 days after RNA transfection of MA/JFH-1.2 and MA/JFH-1.2/R167G at an MOI of 0.005. Core protein levels in medium from MA/JFH-1.2/R167G-infected cells increased with the same kinetics as levels of JFH-1 (Fig. 3E), and the population of core protein-positive cells was almost the same as with JFH-1-infected cells (Fig. 3F), indicating that MA/JFH-1.2/R167G virus spread as rapidly as JFH-1 virus. In contrast, we observed no infectious foci in the MA/JFH-1.2 virus-inoculated cells (Fig. 3F). These data suggest that the R167G mutation in the core region was a cell culture-adaptive mutation and that it enhanced infectious MA/JFH-1.2 virus production.

In order to determine whether R167G enhances RNA replication or other steps in the viral life cycle, we performed a single-cycle virus production assay (11) using Huh7-25 cells, a HuH-7-derived cell line lacking CD81 expression on the cell surface (1).

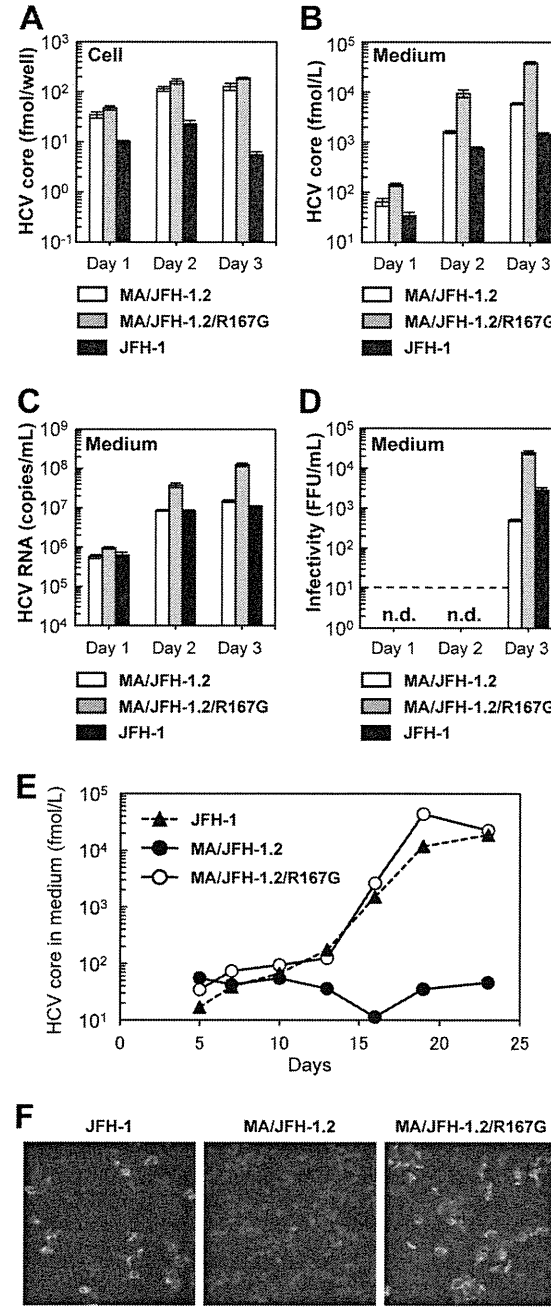

FIG 3 Effects of R167G on replication and virus production of MA/JFH-1.2 in Huh7.5.1 cells. Ten micrograms of HCV RNA was transfected into Huh7.5.1 cells, and cells and medium were harvested on days 1, 2, and 3. HCV core protein levels in the cells (A) and culture medium (B) and HCV RNA levels in the medium (C) and the infectivity of culture medium (D) from HCV RNA-transfected Huh7.5.1 cells are shown. n.d., not determined. Dashed line indicates the detection limit. Assays were performed three times independently, and data are presented as means ± standard deviation. (E) HCV core protein levels in culture medium from cells infected with medium at 3 days posttransfection at an MOI of 0.005. (F) Immunostained cells at 19 days postinfection. Infected cells were visualized with anti-core antibody (green), and nuclei were visualized with DAPI (blue).

This cell line can support replication and infectious virus production upon transfection of HCV genomic RNA but cannot be reinfected by progeny virus, thereby allowing observation of a single cycle of infectious virus production without the confounding ef-

fects of reinfection. R167G did not affect HCV core protein levels in the chimeric RNA-transfected Huh7-25 cells (Fig. 4A), demonstrating that R167G did not enhance RNA replication. Nevertheless, R167G increased HCV core protein levels in the medium ($P < 0.05$ on days 2 and 3) and infectivity (Fig. 4B and C). These results suggest that R167G did not affect RNA replication but affected other steps such as virus assembly and/or virus secretion.

Virus particle assembly efficiency was then assessed by determining intracellular-specific infectivity from infectivity and RNA titer in the cells, as reported previously (11). As shown in Fig. 4G, R167G enhanced intracellular-specific infectivity of MA/JFH-1.2 virus 10.2-fold. Virus secretion efficiency was also calculated from the amount of intracellular and extracellular infectious virus, but R167G had no effect (Fig. 4G).

To confirm the effects of Arg167 in other HCV strains, we tested its effects on JFH-1. As aa 167 of JFH-1 is Gly, we replaced it with Arg (G167R). HCV core protein levels in the cells were not affected by G167R (Fig. 4D), and no effects on RNA replication were confirmed. HCV core protein levels in the medium and infectivity decreased after G167R mutation (Fig. 4E and F). As the G167R mutation decreased intracellular infectious virus production of JFH-1 to undetectable levels, we were unable to determine the intracellular-specific infectivity and virus secretion efficiency of JFH-1 G167R (Fig. 4G). These results indicate that Gly is favored over Arg at core position 167 for infectious virus assembly in multiple HCV strains.

MA harboring the R167G mutation, 5′ UTR, and N3H (NS3 helicase) and N5BX (NS5B to 3′ X) regions of JFH-1 replicated and produced infectious chimeric virus. In order to establish a genotype 2b cell culture system with the MA strain with minimal regions of JFH-1, we attempted to reduce JFH-1 content in MA/JFH-1.2. We previously reported that replacement of the N3H and N5BX regions of JFH-1 allowed efficient replication of the J6CF strain, which normally cannot replicate in cells (21). Thus, we tested whether the N3H and N5BX regions of JFH-1 could also support MA RNA replication.

We prepared two chimeric MA constructs harboring the 5′ UTR and N3H and N5BX regions of JFH-1, MA/N3H+N5BX-JFH1 (Fig. 5A) and MA/N3H+N5BX-JFH1/R167G. After *in vitro* transcribed RNA was transfected into Huh7.5.1 cells, intracellular core protein levels of MA/N3H+N5BX-JFH1 and MA/N3H+N5BX-JFH1/R167G RNA-transfected cells increased in a time-dependent manner and reached almost the same levels as with MA/JFH-1.2 RNA-transfected cells on day 5 (Fig. 5B). Extracellular core protein and HCV RNA levels of MA/N3H+N5BX-JFH1 and MA/N3H+N5BX-JFH1/R167G RNA-transfected cells also increased in a time-dependent manner (Fig. 5C and D). However, they were more than 10 times lower than with MA/JFH-1.2 RNA-transfected cells although intracellular core levels were comparable on day 5 (Fig. 5B to D).

We then tested whether the medium from MA/N3H+N5BX-JFH1 and MA/N3H+N5BX-JFH1/R167G RNA-transfected cells was infectious. Infectivity of the medium from MA/N3H+N5BX-JFH1 RNA-transfected cells was below the detection limit, and that of MA/N3H+N5BX-JFH1/R167G RNA-transfected cells on day 5 was very low ($3.3 \times 10^1 \pm 2.1 \times 10^1$ FFU/ml) (Fig. 5E). To confirm infectivity, the culture media were concentrated, and their infectivity was determined. Infected foci were observed after infection with concentrated medium in MA/N3H+N5BX-JFH1/R167G RNA-transfected cells (Fig. 5F), and infectivity was found

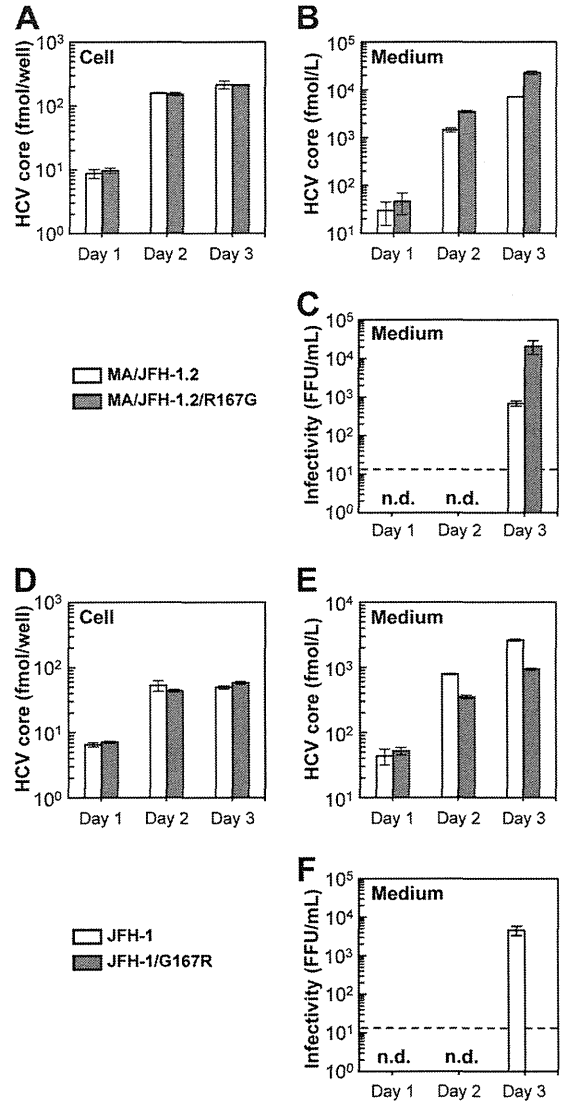

G

Construct	Intracellular Specific Infectivity (FFU/ x10^5 HCV RNA copies)	Infectious Virus Secretion (Extra/Intra)
MA/JFH-1.2	1.68 ± 0.404	20.2 ± 4.26
MA/JFH-1.2/R167G	17.1 ± 4.38	14.1 ± 1.65
JFH-1	1.78 ± 0.364	63.3 ± 6.44
JFH-1/G167R	NA	NA

FIG 4 Effects of R167G on replication and virus production of MA/JFH-1.2 and JFH-1 in Huh7-25 cells. Ten micrograms of HCV RNA was transfected into Huh7-25 cells, and cells and medium were harvested on days 1, 2, and 3. HCV core protein levels in cells (A and D) and in medium (B and E) were measured, and infectivity of medium (C and F) was determined. n.d., not determined. Dashed line indicates the detection limit. (G) Intracellular specific infectivity and virus secretion efficiency of chimeric HCV RNA-transfected cells. Intracellular and extracellular infectivity of day 3 samples was determined, and specific infectivity and virus secretion rate were calculated. Assays were performed three times independently, and data are presented as means ± standard deviation. NA, not available.

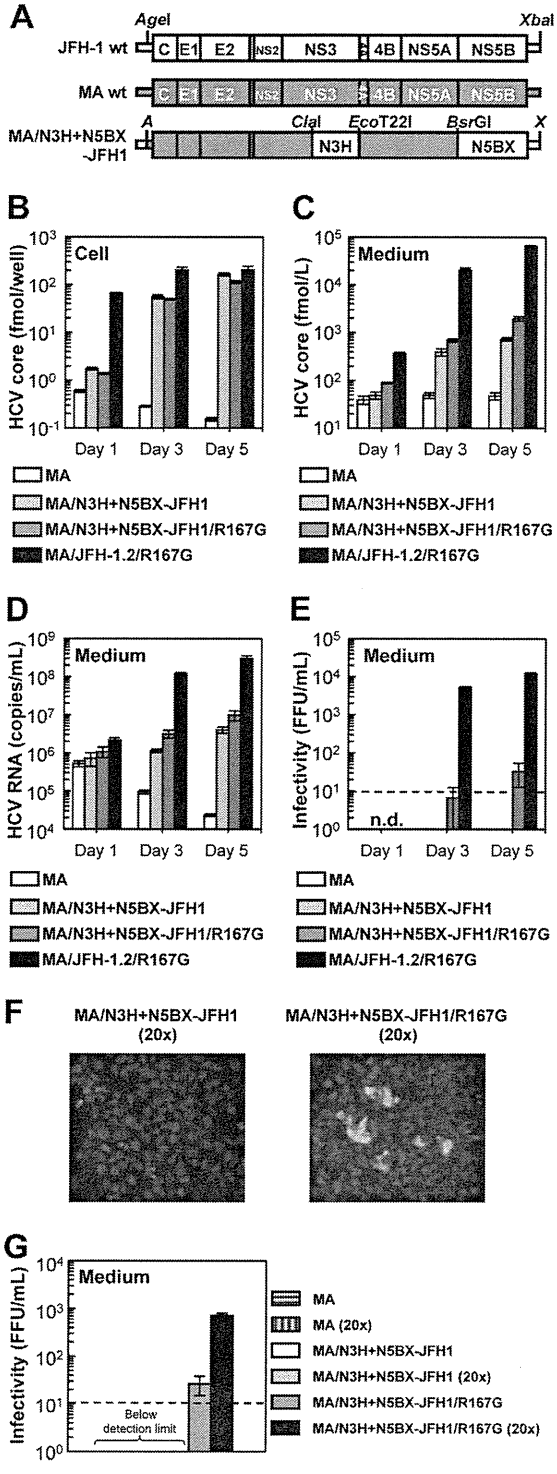

FIG 5 Replication and virus production of MA/N3H+N5BX-JFH1/R167G in Huh7.5.1 cells. (A) Schematic structures of JFH-1, MA, and MA/N3H+N5BX-JFH1. The junction of JFH-1 and MA in the 5′ UTR is an AgeI site; the junctions of MA and JFH-1 in the NS3 regions are ClaI and EcoT22I sites, and the junction in the NS5B region is a BsrGI site. A, AgeI; X, XbaI. (B to G) Chimeric HCV RNA replication in Huh7.5.1 cells. Ten micrograms of HCV RNA was transfected into Huh7.5.1 cells, and cells and medium were harvested on days 1, 3, and 5. HCV core protein levels in cells (B) and in medium (C) and HCV RNA levels in medium (D) were measured, and infectivity of medium (E) was determined. Assays were performed three times independently, and data are presented as means ± standard deviation. n.d., not determined. Dashed line indicates the detection limit. (F) Immunostained cells. Huh7.5.1 cells were infected with concentrated medium from RNA-transfected cells on day 5. Infected cells were visualized with anti-core antibody (green), and nuclei were visualized with DAPI (blue). (G) Infectivity of concentrated culture medium from HCV RNA-transfected cells. Culture medium was concentrated by 20 times. Infectivities of original and concentrated culture media were determined. Dashed line indicates detection thelimit.

to be $7.27 \times 10^2 \pm 7.57 \times 10^1$ FFU/ml (Fig. 5G). No infected foci were observed after infection of MA/N3H+N5BX-JFH1 RNA-transfected cells, even when medium was concentrated (Fig. 5F), although intracellular and extracellular core protein levels were comparable to those with MA/N3H+N5BX-JFH1/R167G RNA-transfected cells (Fig. 5B and C). These results indicate that replacement of the 5′ UTR and N3H and N5BX regions in JFH-1 were necessary to rescue autonomous replication in the replication-incompetent MA strain and for secretion of infectious chimeric virus. However, the secretion and infection efficiencies of the virus were low.

Cell culture-adaptive mutations enhanced infectious virus production of MA/N3H+N5BX-JFH1/R167G. Because MA/N3H+N5BX-JFH1/R167G replicated efficiently but produced very small amounts of infectious virus, we performed a long-term culture of the RNA-transfected cells in order to induce cell culture-adaptive mutations that could enhance infectious virus production. We prepared RNA-transfected cells using two constructs, MA/N3H+N5BX-JFH1 and MA/N3H+N5BX-JFH1/R167G; both of these replicated efficiently, and MA/N3H+N5BX-JFH1/R167G produced infectious virus at low levels while MA/N3H+N5BX-JFH1 did not. Immediately after transfection, the HCV core protein levels in the medium of each RNA-transfected cell culture peaked at 3.0×10^3 fmol/liter and declined thereafter. However, the core protein level in the medium with MA/N3H+N5BX-JFH1/R167G RNA-transfected cells continued to increase and reached a peak of 2.7×10^5 fmol/liter 54 days after transfection, at which point most cells were core protein positive (Fig. 6B). The core protein level in the medium with MA/N3H+N5BX-JFH1 RNA-transfected cells did not increase and core-positive cells were scarce on day 54 (Fig. 6B). We analyzed the viral genome in the culture supernatants from day 54 for possible mutations and identified four nonsynonymous mutations in the MA/N3H+N5BX-JFH1/R167G genome: L814S (NS2), R1012G, (NS2), T1106A (NS3), and V1951A (NS4B). In order to test whether these amino acid substitutions enhance infectious virus production, L814S, R1012G, T1106A, and V1951A were introduced into MA/N3H+N5BX-JFH1/R167G, and the product was designated MA/N3H+N5BX-JFH1/5am (where am indicates adaptive mutation). On day 1, although HCV core protein levels in the MA/N3H+N5BX-JFH1/5am RNA-transfected cells were higher than those of MA/N3H+N5BX-JFH1/R167G RNA-transfected cells, they were still lower than those of MA/JFH-1.2/R167G RNA-transfected cells; however, on days 3 and 5, they reached a level comparable to that of MA/JFH-1.2/R167G RNA-transfected cells (Fig. 6C). HCV core protein and HCV RNA levels in the medium of MA/N3H+N5BX-JFH1/5am RNA-transfected cells were higher than those of MA/JFH-1.2/R167G RNA-transfected cells ($P < 0.05$, Fig. 6D and 6E, respectively). MA/N3H+N5BX-JFH1/5am, containing the four additional adaptive mutations, produced infectious virus at the same level as MA/JFH-1.2/R167G on day 5 (Fig. 6F). These results indicate that the

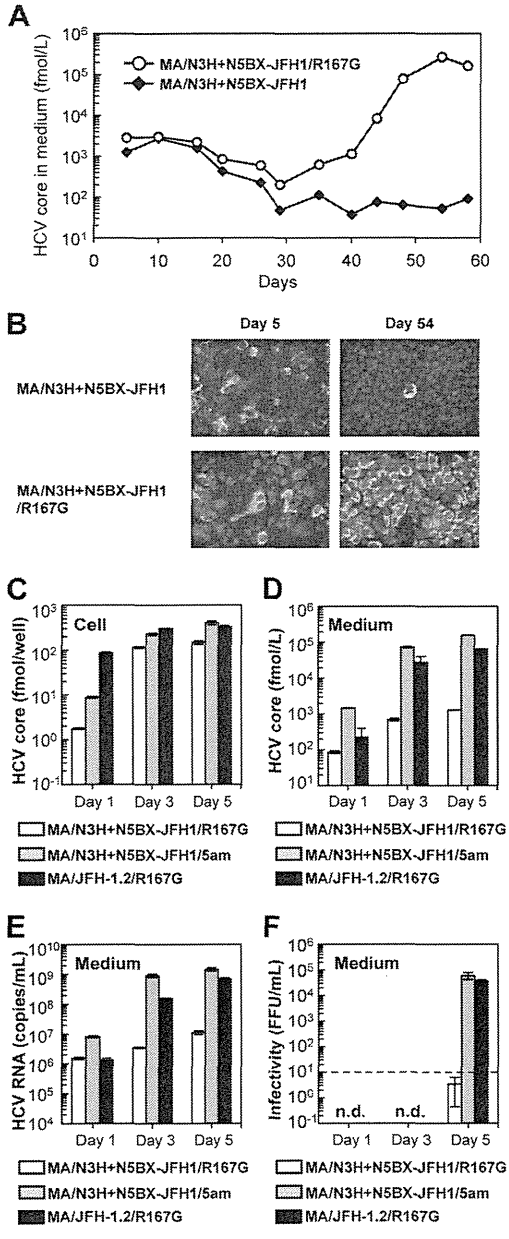

FIG 6 Cell culture-adaptive mutations enhanced infectious virus production of MA/N3H+N5BX-JFH1/R167G. (A) Long-term culture of MA/N3H+N5BX-JFH1 and MA/N3H+N5BX-JFH1/R167G RNA-transfected cells. Ten micrograms of HCV RNA was transfected into Huh7.5.1 cells, and cells were passaged every 2 to 5 days, depending on cell status. Culture medium was collected after every passage, and HCV core protein levels were measured. HCV core protein levels in culture medium from MA/N3H+N5BX-JFH1 and MA/N3H+N5BX-JFH1/R167G RNA-transfected cells are presented. (B) Immunostained cells on days 5 and 54 after transfection. Infected cells were visualized with anti-core antibody (green), and nuclei were visualized with DAPI (blue). (C to F) Effect of four additional cell culture-adaptive mutations on virus production. Ten micrograms of HCV RNA was transfected into Huh7.5.1 cells, and cells and medium were harvested on days 1, 3, and 5. HCV core levels in cells (C) and in medium (D) and HCV RNA levels in medium (E) were measured, and infectivity of medium (F) was determined. Assays were performed three times independently, and data are presented as means ± standard deviation. n.d., not determined. Dashed line indicates the detection limit.

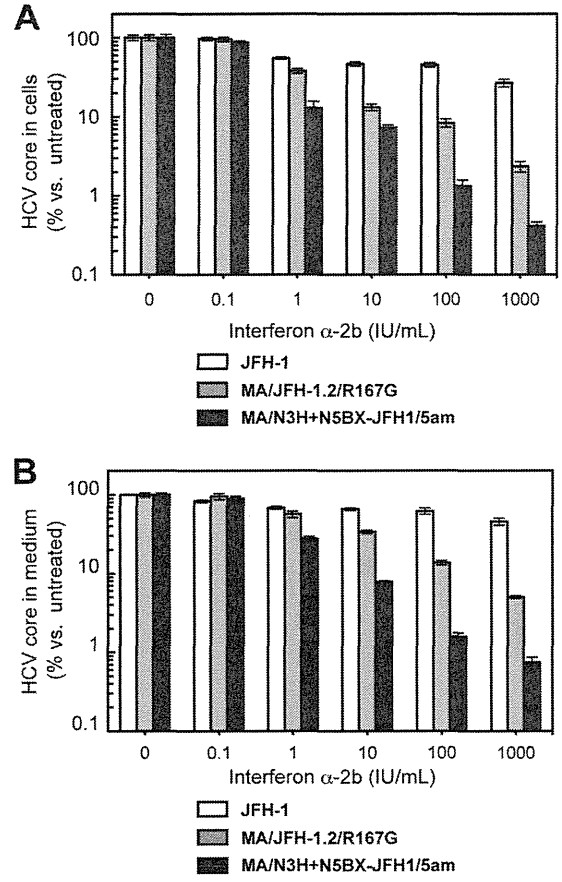

FIG 7 Comparisons of interferon sensitivity between JFH-1, MA/JFH-1.2/R167G and MA/N3H+N5BX-JFH1/5am. Two micrograms of HCV RNA was transfected into Huh7.5.1 cells, and interferon was added at the indicated concentrations at 4 h after transfection. HCV core protein levels in cells (A) and in medium (B) on day 3 were measured, and data are expressed as percent versus untreated cells (0 IU/ml). Assays were performed three times independently, and data are presented as means ± standard deviation.

four additional adaptive mutations enhance infectious virus production and that MA/N3H+N5BX-JFH1/5am RNA-transfected cells replicate and produce infectious virus as efficiently as MA/JFH-1.2/R167G RNA-transfected cells.

Comparison of interferon sensitivity between JFH-1, MA/JFH-1.2/R167G, and MA/N3H+N5BX-JFH1/R167G. Using the newly established genotype 2b infectious chimeric virus, we compared interferon sensitivity between the JFH-1, MA/JFH-1.2/R167G, and MA/N3H+N5BX-JFH1/5am viruses. JFH-1 or MA chimeric viral RNA-transfected Huh7.5.1 cells were treated with 0.1, 1, 10, 100, or 1,000 IU/ml interferon α-2b, and HCV core protein levels in the cells and in culture media were compared. Interferon decreased HCV core protein levels in the JFH-1 RNA-transfected cells and in the medium in a dose-dependent manner, and production was inhibited to 26.8% ± 3.0% and 45.6% ± 4.7%, respectively, of control levels (Fig. 7A and B, respectively). In contrast, HCV core protein levels in cells and medium of MA/JFH-1.2/R167G and MA/N3H+N5BX-JFH1/5am RNA-transfected cells decreased more pronouncedly in a dose-dependent manner (Fig. 7A and B, respectively). HCV core protein levels in cells and medium from MA/N3H+N5BX-JFH1/5am RNA-transfected cells were lower than those from MA/JFH-1.2/